

# Surface-enhanced resonant Raman spectroscopy of single-wall carbon nanotubes adsorbed on silver and gold surfaces

P. Corio, S. D. M. Brown, and A. Marucci

*Department of Physics, Massachusetts Institute of Technology, Cambridge, Massachusetts 02139*

M. A. Pimenta

*Departamento de Física, Universidade Federal de Minas Gerais, Caixa Postal 702, 30123-970 Belo Horizonte, Brazil*

K. Kneipp

*George R. Harrison Spectroscopy Laboratory, Massachusetts Institute of Technology, Cambridge, Massachusetts 02139  
and Department of Physics, Technical University of Berlin, D-10623 Berlin, Germany*

G. Dresselhaus

*Francis Bitter Magnet Laboratory, Massachusetts Institute of Technology, Cambridge, Massachusetts 02139*

M. S. Dresselhaus

*Department of Electrical Engineering and Computer Science and Department of Physics, Massachusetts Institute of Technology, Cambridge, Massachusetts 02139*

(Received 25 October 1999)

The surface-enhanced resonant Raman-scattering (SERRS) spectra of single-walled carbon nanotubes (SWNT's) adsorbed on silver and gold metal island films and on colloidal silver cluster substrates were investigated using different laser excitation wavelengths. The observed enhancement in the SERRS signal of the SWNT's results from: (i) an "electromagnetic" surface-enhanced Raman spectral (SERS) enhancement due to resonances between optical fields and the electronic excitations in the metallic nanostructures, (ii) a "chemical" SERS enhancement due to the interaction between the SWNT's and the metal surfaces, and (iii) a selective resonance Raman effect between the incident and scattered photons and electronic transitions between the one-dimensional van Hove singularities in the electronic density of states of metallic and semiconducting nanotubes. We have observed changes in the relative intensities and shifts in the peak frequencies of several vibrational modes of the SWNT's upon adsorption on a metal surface, which indicate a specific interaction of the nanotubes with the metal surface. Changes in the resonant Raman spectra due to interaction with the silver or gold surfaces are apparent in the second-order Raman bands, especially in the dispersive features, such as the second-order Raman  $G'$  band, which upshifts in the SERRS spectra relative to the resonant Raman-scattering (RRS) spectra, providing evidence for a significant perturbation of the electronic levels for the adsorbed nanotubes. In addition, the SERRS spectra show an additional enhancement of the Raman signal for specific features in the vibrational spectra of the metallic nanotubes, in contrast to the case for the semiconducting nanotubes for which the normal RRS and SERRS spectral profiles are very similar. These results can be explained in terms of a specific charge-transfer enhancement effect for the metallic nanotubes.

## I. INTRODUCTION

Resonance Raman spectroscopy provides a sensitive probe of both the vibrational and electronic properties of carbon nanotubes.<sup>1-4</sup> Furthermore, surface-enhanced Raman spectroscopy (SERS) can enhance the Raman scattering of species adsorbed on specially prepared metal surfaces by many orders of magnitude, thereby providing a means for observing Raman spectra for single molecules.<sup>5,6</sup> Single-wall carbon nanotubes (SWNT's) can show a strong surface-enhanced Raman effect when they are in contact with metallic structures with nanometer sized roughness.<sup>7,8</sup> The strong enhancement of the Raman signal by SERS opens up exciting opportunities for studying the Raman spectrum of a small number of nanotubes, and, maybe, even a single nanotube, to retrieve the intrinsic properties of SWNT's, which in con-

ventional Raman experiments are hidden under the inhomogeneous broadening coming from ensemble averaging.

The dominant contribution to the enhancement of the Raman signal comes from strongly enhanced optical fields in the vicinity of the metallic nanostructures (electromagnetic SERS enhancement).<sup>9,10</sup> In general, the SERS enhancement can also have a contribution from a so-called "chemical" SERS enhancement mechanism,<sup>9-12</sup> which is based on the specific interaction between the target molecule and the metal substrate, in our case, the interaction between the nanotube and the "SERS-active" metal, which takes place in the extremely strong optical fields around the metallic nanostructure. This enhancement effect is based on changes or improvements in the resonant Raman-scattering (RRS) conditions in the "new system" consisting of nanotube, metal substrate and photon, compared to the usual "system"

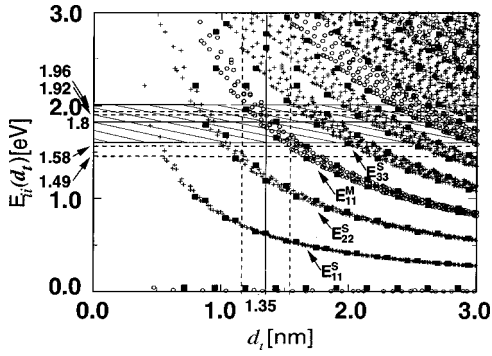


FIG. 1. Calculation (Refs. 21, 32, and 33) for  $\gamma_0 = 2.9$  eV of the energy separations  $E_{ii}(d_t)$  for all  $(n, m)$  nanotube values vs nanotube diameter  $0.7 < d_t < 3.0$  nm. Semiconducting and metallic nanotubes are indicated by crosses and open circles, respectively. The filled squares denote zigzag tubes. The vertical lines denote  $d_t = 1.35 \pm 0.20$  nm for our single-wall carbon nanotube sample. The cross-hatch pattern denotes the range in  $E_{\text{laser}}$  where metallic nanotubes are expected to contribute resonantly to both the Stokes and anti-Stokes spectra.

consisting of nanotube and photon, which is studied in “normal” RRS.<sup>3,4,13</sup>

Previous work has concentrated on the estimate of the total SERS enhancement factor when the carbon nanotubes are adsorbed on silver colloidal clusters.<sup>7</sup> In the present work, we focus on the nature of the so-called “chemical contribution” to the SERS enhancement, which is based on the electronic interaction between the nanotubes and the metallic substrate. In particular, the dependence of this interaction on the metal surface, and on the laser excitation energy is studied in the present work.

In the case of carbon nanotubes, which show a strong resonance Raman effect associated with the singularities in the one-dimensional (1D) electronic density of states,<sup>3,4</sup> the sensitivity of the SERS probe can be especially high, since the enhancement effects from both the resonance Raman and SERS effects can be combined multiplicatively for laser excitation wavelengths in the visible/near-infrared spectral region.

Surface-enhanced Raman scattering studies under resonance Raman-scattering conditions, denoted here by SERRS, when applied to SWNT’s, open up very interesting opportunities to study the “chemical” SERS effect, since a nanotube sample provides “target molecules,” which have well defined, and even different [semiconducting (S) and metallic (M)] electronic structures, as illustrated in Fig. 1, where interband transitions between van Hove singularities in the 1D density of states of the valence and conduction bands are shown for semiconducting (S) and metallic (M) nanotubes. In our paper we investigate the chemical contribution to the SERRS effect of SWNT’s. We apply different excitation wavelengths in order to probe the electronic density of states for metallic and semiconducting nanotubes by measuring the excitation profiles (Raman scattering vs excitation energy) of the tangential  $G$  modes. Moreover, frequency shifts of the  $G'$  band, which appears at  $\approx 2600 \text{ cm}^{-1}$  in the second-order spectra of the nanotubes, provide us with an independent probe of the nanotube-metal interaction.

In this paper we investigate a number of issues relevant to surface-enhanced Raman spectroscopy (SERS) of single-

wall nanotubes under resonance Raman conditions. Resonant Raman-scattering (RRS) spectra are compared with the corresponding SERRS spectra for six laser excitation energies  $E_{\text{laser}}$  for Au and Ag films and for nanostructured Ag cluster substrates for several distinct spectral features in the Raman spectra. A plot of the interband transitions between van Hove singularities in the 1D density of states in the valence and conduction bands for semiconducting and metallic nanotubes (Fig. 1) is used to interpret and compare the detailed features in the RRS and SERS spectra. The selective enhancement of specific features in the Raman spectra is investigated for both semiconducting and metallic nanotubes for various  $E_{\text{laser}}$  values, by carrying out detailed line-shape analysis of these spectra. Additional understanding of the resonant SERS enhancement processes is achieved through comparison of the RRS and SERRS anti-Stokes spectra. To extract information about the interaction mechanism between the nanotubes and metal substrates, we have studied the mode frequencies and intensities of the  $G'$  band, which is associated with a resonant second-order process for phonons near the  $K$  point in the 2D graphene Brillouin zone. From these studies we obtained detailed information about the comparative roles of the electromagnetic and charge-transfer SERS enhancement mechanisms for metallic and semiconducting nanotubes.

## II. EXPERIMENTAL DETAILS

The single-walled carbon nanotubes used in this study were produced through the arc discharge method and had a diameter distribution of  $d_t = 1.35 \pm 0.20$  nm. The Raman and SERS experiments were performed under ambient conditions using a backscattering configuration. For laser excitation radiation we used the 514.5-nm (2.41-eV) line from an  $\text{Ar}^+$  laser; the 632.8-nm (1.96-eV) line from an air cooled He-Ne laser; the 647.1-nm (1.92-eV) and 676.4-nm (1.83-eV) lines from a  $\text{Kr}^+$  laser; the 782.0-nm (1.58-eV) line of a solid-state Al-doped GaAs laser; and the 830-nm (1.49-eV) line of a Ti:sapphire laser.

The SERS substrates were prepared by vacuum evaporation of silver (film thicknesses of 50 and 100 Å) or gold (film thickness of 50 Å) on to glass slides. The nanotubes were deposited on the rough metal surface from a dispersion prepared by sonication of the nanotubes suspended in isopropanol. SERS experiments were also carried out using silver colloidal solutions, prepared according to a previously described procedure.<sup>7,14</sup> A solution of nanotubes in isopropanol at extremely low nanotube concentrations was added to the silver aqueous colloidal solution. For the measurements, a droplet of this sample solution was evaporated on a glass slide, resulting in the placement of fractal colloidal silver structures in close contact with some of the single-wall nanotubes.

The extinction (absorbance) spectra for the prepared SERS substrates in the absence of the nanotubes are shown in Fig. 2. For the silver film, the surface plasmon absorption gives rise to a broad band between 400 and 900 nm, while the absorption band for the gold island film starts at  $\sim 500$  nm, and extends to the near-infrared region. The very broad extinction (absorption) bands observed for both the Ag and Au substrates are characteristic of the presence of clusters of metal particles, since the single metal particle absorption for

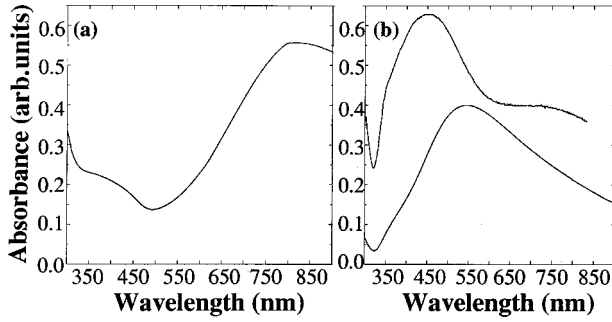


FIG. 2. Absorbance spectra of (a) a 50-Å gold film and (b) a 100-Å silver film deposited on a glass substrate (lower curve), and fractal colloidal silver clusters in aqueous substrate (upper curve).

silver and gold is known to give rise to narrower bands at about 400 and 520 nm, respectively.<sup>15</sup> The differences in the spectra between colloidal silver particles and evaporated silver film substrates arise from the different distributions of particle sizes within the clusters in the two kinds of silver substrates.

### III. RESULTS AND DISCUSSION

Figure 3 shows a comparison, over a broad frequency range from 500–3500  $\text{cm}^{-1}$ , between the normal [Fig. 3(a)] and surface-enhanced resonant Raman spectra observed from single wall carbon nanotubes (SWNT's) on a silver film [Fig. 3(b)] and on a gold film [Fig. 3(c)]. These spectra were measured using 632.8-nm (1.96-eV) excitation and using 40-W/ $\text{cm}^2$  incident laser intensity. The spectra have all been corrected for the spectral response of the system.

As shown in Fig. 1, a strong contribution to the Stokes Raman scattering process at a laser excitation energy  $E_{\text{laser}} = 1.96$  eV for nanotube diameters  $d_t = 1.35 \pm 0.20$  nm comes from resonance with electronic transitions between the highest energy singularity in the 1D density of electronic states in the valence band to the corresponding lowest energy singularity in the conduction band for *metallic* nanotubes, denoted

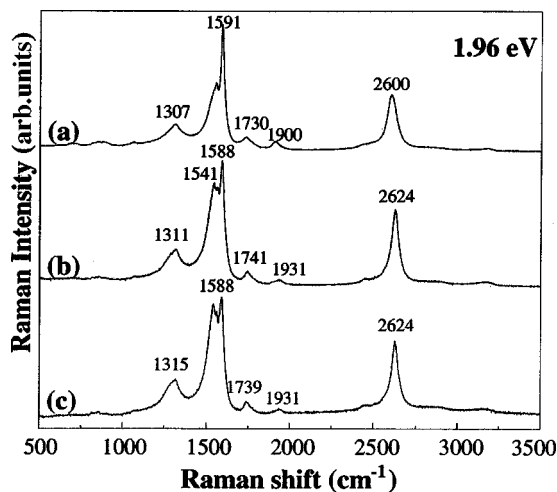


FIG. 3. Normal resonant Raman-scattering (RRS) spectrum (a), and surface enhanced resonant Raman-scattering (SERRS) spectra of single-wall nanotubes (SWNT's) adsorbed on (b) gold and (c) silver island films in the 500–3500- $\text{cm}^{-1}$  range using laser excitation at  $E_{\text{laser}} = 632.8$  nm (1.96 eV).

by  $E_{11}^M(d_t)$ . Figure 1 indicates that a strong resonant contribution for the Stokes process also occurs from *semiconducting* nanotubes within the SWNT sample, with diameters  $d_t$  in the upper range of the  $d_t$  distribution, mainly through resonance of the scattered photons with the  $E_{33}^S(d_t)$  electronic transition (see Fig. 1).<sup>3,16,17</sup> [The superscripts M and S in  $E_{ii}(d_t)$  refer to metallic and semiconducting nanotubes, respectively.]

The dominant feature in the spectra in Fig. 3 is associated with the first-order tangential band occurring in the phonon frequency range 1500–1600  $\text{cm}^{-1}$ . From the line shape of this broad Raman band,<sup>3,4</sup> we infer that the dominant contribution to the spectrum comes from metallic nanotubes. We identify features of lower intensity near 1310  $\text{cm}^{-1}$  with the so-called *D* band, associated with phonons near the *K* point in the 2D graphene Brillouin zone.<sup>18</sup> The feature in the 1730–1740- $\text{cm}^{-1}$  range is tentatively associated with a combination mode<sup>16</sup> between the tangential mode and the radial breathing mode phonons ( $\omega_{\text{tang}} + \omega_{\text{RBM}}$ ), while the feature in the 1900–1930- $\text{cm}^{-1}$  range is tentatively attributed to a combination mode<sup>16</sup> ( $\omega_{\text{tang}} + 2\omega_{\text{RBM}}$ ). A weak feature near 2440  $\text{cm}^{-1}$  (only observed at higher magnification) is identified with a nonresonant overtone in the second-order spectrum of the *K*-point vibration at about 1220  $\text{cm}^{-1}$ ,<sup>16</sup> and finally the strong feature in the 2600–2624  $\text{cm}^{-1}$  range is due to the *G'* band which occurs as an overtone of the *D*-band feature at twice the *D*-band frequency. Both the *D* band and the *G'* band are associated with a strong electron-phonon coupling near the *K* point in the 2D Brillouin zone when the phonon and electron wave vectors are equal,<sup>18,19</sup> while the other features in the spectrum in Fig. 3 are identified with phonons near  $k=0$  (the  $\Gamma$  point) in the Brillouin zone for the nanotubes. At a given value of  $E_{\text{laser}}$ , all nanotubes contribute to the *G'* band, while only those nanotubes with electronic transitions (see Fig. 1) that are in resonance with the incident and/or scattered photon contribute significantly to the tangential band spectrum.

Figure 3 shows that qualitatively similar spectral features are observed for the Stokes process for normal resonant Raman scattering and for SERRS, though there are differences in the detailed line shape, peak frequencies, and relative intensities between the RRS and SERRS spectra for either of the two metal substrates, as discussed below. The SERRS spectra for the Ag and Au films are almost identical. Generally speaking, the features which show little dispersion (dependence of the Raman frequency on  $E_{\text{laser}}$ ) in the RRS spectra show very small frequency shifts between features in the RRS spectra and in the corresponding SERRS spectra. In contrast, features, such as those associated with the *D* band, the  $\omega_{\text{tang}} + 2\omega_{\text{RBM}}$  combination mode, and the *G'* band, which all show large dispersion in their RRS spectra, also show large differences between their RRS and SERRS spectra at a fixed  $E_{\text{laser}}$ . These differences in the spectral features between the RRS and SERRS spectra are a main focus of this paper, as discussed in more detail in the next section.

#### A. Tangential Raman band

To provide a more detailed comparison between the RRS and SERRS spectra, we show in Fig. 4 the tangential band in the Stokes spectra as observed by RRS for five different

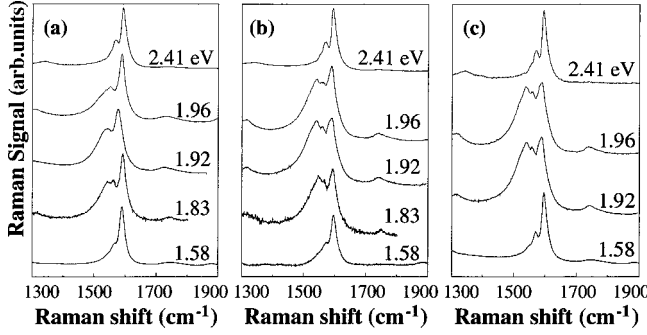


FIG. 4. The spectral region between 1300–1900  $\text{cm}^{-1}$  in more detail showing the RRS spectrum (a), and the SERRS spectra for SWNT's adsorbed on (b) a 50-Å gold film and (c) a 100-Å silver film for several laser excitation energies  $E_{\text{laser}}$ .

$E_{\text{laser}}$  values (a), by SERRS with a 50-Å Au film for five different  $E_{\text{laser}}$  values (b), and by SERRS with a 100-Å Ag film for four different  $E_{\text{laser}}$  values (c). Regarding the tangential band between 1500–1630  $\text{cm}^{-1}$ , semiconducting nanotubes dominate the Stokes spectra at  $E_{\text{laser}}=1.58$  and 2.41 eV, metallic nanotubes dominate the spectra at  $E_{\text{laser}}=1.83$  and 1.92 eV, while the spectra at 1.96 eV are in an interesting regime where both metallic and semiconducting tubes contribute strongly. Comparison of the Raman spectra for a given  $E_{\text{laser}}$  value shows that the SERRS spectra for the two different metal film substrates are more similar to one another, than are the RRS and SERRS spectra at the same  $E_{\text{laser}}$  value. To make a comparison between the three spectra more quantitative, we carried out a Lorentzian line-shape analysis for the various spectra in Fig. 4. The results of this analysis are summarized in Table I, and are shown for illustration in Fig. 5 for  $E_{\text{laser}}=1.96$  eV. We now discuss these results in more detail.

For the two laser excitation energies where only semiconducting nanotubes contribute to the resonant Stokes spectra,  $E_{\text{laser}}=1.58$  eV [resonant with the  $E_{22}^S(d_t)$  electronic transition for semiconducting nanotubes (see Fig. 1)] and 2.41 eV [resonant with  $E_{33}^S(d_t)$ ],<sup>16,20,21</sup> the tangential phonon mode region shows Lorentzian components at 1563, 1591, and 1601  $\text{cm}^{-1}$  (see Table I), which are associated with normal resonant Raman spectra from semiconducting nanotubes,<sup>3</sup> as shown in Fig. 1. The SERRS spectra at  $E_{\text{laser}}=1.58$  and 2.41 eV for both Ag and Au film substrates are closely similar to each other and to the normal Raman spectra, and basically the same frequencies and relative intensities can be observed for the three constituent Lorentzian components, as indicated in Table I. Below we describe SERRS and RRS spectra taken at  $E_{\text{laser}}=1.49$  eV under different experimental conditions, and using a fractal colloidal silver substrate, again yielding the same Stokes spectra for semiconducting SWNT's (see Fig. 6), namely that the relative intensities of the three dominant Lorentzian components are very similar for the SERRS and RRS Stokes spectra for *semiconducting* SWNT's.

For the three values of  $E_{\text{laser}}$  in Fig. 4 within the  $1.8 < E_{\text{laser}} < 2.0$  eV range, the RRS spectra show the appearance of different Lorentzian components at 1515, 1540, and 1581  $\text{cm}^{-1}$ , which can be identified (see Fig. 1) with resonantly enhanced features from metallic nanotubes in resonance with

TABLE I. Frequencies ( $\omega$ ), full width at half maximum intensity ( $\Gamma$ ) of the Lorentzian curves, and the intensities of each Lorentzian component for the tangential bands relative to the 1591- $\text{cm}^{-1}$  peak as a function of  $E_{\text{laser}}$  for the Stokes spectra. The symbols ( $m$ ) and ( $sc$ ) refer to components associated with metallic and semiconducting nanotubes, respectively.

$\omega$ ( $\text{cm}^{-1}$ )	$\Gamma$ ( $\text{cm}^{-1}$ )	RRS Rel. int.	SERS Au Rel. int.	SERS Ag Rel. int.
$E_{\text{laser}}=1.83$ eV				
1515 $m$	53	0.8	1.9	
1540 $m$	41	2.0	2.8	
1563 $sc$	24	0.6	0.5	
1581 $m$	24	1.2	1.3	
1591 $sc$	15	1.0	1.0	
1601 $sc$	34	0.6	0.7	
$E_{\text{laser}}=1.92$ eV				
1515 $m$	53	1.1	1.9	1.7
1540 $m$	41	2.5	2.9	2.8
1563 $sc$	24	0.7	0.5	0.5
1581 $m$	24	1.2	1.2	1.2
1591 $sc$	15	1.0	1.0	1.0
1601 $sc$	34	0.6	0.7	0.7
$E_{\text{laser}}=1.96$ eV				
1515 $m$	53	0.72	1.9	1.8
1540 $m$	41	1.1	2.7	2.9
1563 $sc$	24	0.4	0.5	0.5
1581 $m$	24	1.1	1.3	1.2
1591 $sc$	15	1.0	1.0	1.0
1601 $sc$	34	0.4	0.6	0.55
$E_{\text{laser}}=2.41, 1.58$ eV				
1563 $sc$	24	0.6	0.6	0.6
1591 $sc$	15	1.0	1.0	1.0
1601 $sc$	34	0.6	0.6	0.6

the  $E_{11}^M(d_t)$  transition.<sup>3</sup> In this laser excitation energy range, significant changes can be seen when comparing the RRS spectra to the two corresponding SERRS spectra, whereas the SERRS spectra for nanotubes on Au and Ag are similar to one another. In particular, the line-shape analysis in Fig. 5 at  $E_{\text{laser}}=1.96$  eV shows that the contributions of certain Lorentzian components for the metallic nanotubes are much more pronounced for the SERRS spectra than for the RRS spectrum, though the peak frequencies for these three metallic components appear to be the same. The SERRS enhancement at  $E_{\text{laser}}=1.96$  eV is particularly strong for the 1540- $\text{cm}^{-1}$  metallic component (150% increase compared to the 1540- $\text{cm}^{-1}$  component in the RRS spectrum), and for the 1515- $\text{cm}^{-1}$  metallic component (160% increase), while the 1581- $\text{cm}^{-1}$  component shows less difference (only  $\sim 15\%$  increase) between the RRS and SERRS spectra. For  $E_{\text{laser}}=1.83$  and 1.92 eV, which are both within the metallic win-

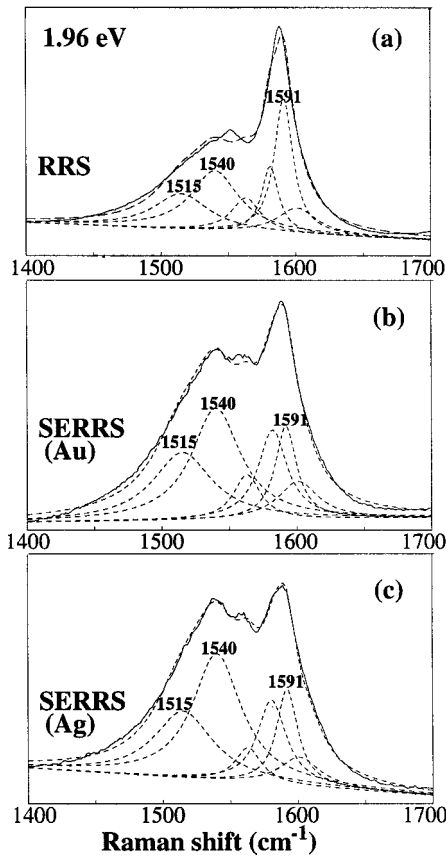


FIG. 5. Deconvolved spectra of the tangential vibrational band obtained with laser excitation ( $E_{\text{laser}}$ ) at 632.8 nm (1.96 eV) for (a) normal resonant Raman spectroscopy, (b) SERRS on an Au substrate, (c) SERRS on an Ag substrate. A Lorentzian analysis of the spectra is made into the same Lorentzian oscillators at 1515, 1540, and 1580- $\text{cm}^{-1}$  for the metallic nanotubes and at 1563, 1591, and 1601  $\text{cm}^{-1}$  for the semiconducting nanotubes (see Table I). The two dominant components in the metallic nanotube regime (at 1515 and 1540  $\text{cm}^{-1}$ ) and the strongest component in the semiconducting nanotube regime (at 1591  $\text{cm}^{-1}$ ) are labeled.

For this sample, the SERRS and RRS spectra can be fit with the same Lorentzian oscillators as for the spectra at  $E_{\text{laser}} = 1.96$  eV, discussed above, and once again the Lorentzian components at 1540 and 1515  $\text{cm}^{-1}$  associated with the metallic nanotubes are more strongly enhanced in the SERRS spectra. The experimental intensity ratios are given explicitly in Table I for various excitation energies and for the relevant Lorentzian oscillators at that value of  $E_{\text{laser}}$ . Table I shows that the phonon modes at 1540 and 1515  $\text{cm}^{-1}$  are enhanced in the SERRS spectra relative to the RRS spectra, while the intensity of the 1581- $\text{cm}^{-1}$  component is almost unchanged. In the spectra at  $E_{\text{laser}} = 1.96$ , 1.92, and 1.83 eV, the relative intensities of the weaker components at 1563, 1591, and 1601  $\text{cm}^{-1}$ , that are associated with the semiconducting nanotubes, are almost the same for the RRS and SERRS spectra. At a given value of  $E_{\text{laser}}$ , the SERRS spectra for the metallic nanotubes are about equally enhanced (within experimental error) for the silver and gold substrates, as shown in Table I. On the other hand, the contributions to the spectra from the semiconducting nanotubes (at 1563, 1591, and 1601  $\text{cm}^{-1}$ ) are essentially the same for

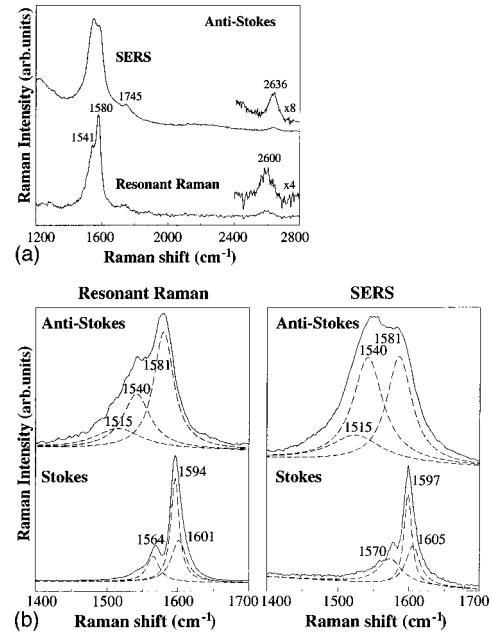


FIG. 6. (a) Anti-Stokes resonant Raman and SERS spectra of SWNT's adsorbed on colloidal silver particles taken with laser excitation at  $E_{\text{laser}} = 1.49$  eV. (b) Lorentzian line-shape analysis of the anti-Stokes tangential vibrational band. The Stokes spectra at  $E_{\text{laser}} = 1.49$  eV are also shown for comparison.

SERRS as compared to RRS, and are also the same for the Ag and Au substrates for all values of  $E_{\text{laser}}$  shown in Table I.

Further information is obtained by comparison of the *anti-Stokes* RRS and SERRS spectra of the SWNT's. To obtain sufficient intensity to observe the SERRS anti-Stokes spectra, fractal colloidal silver clusters were used for the "SERS-active" substrate, exploiting the very high effective enhancement factors (on the order of  $10^{12}$ ) recently reported for nanotubes adsorbed on such silver surface when excited at 830 nm ( $E_{\text{laser}} = 1.49$  eV).<sup>7</sup> In general, due to Boltzmann population considerations, the intensity of the anti-Stokes signal of the tangential modes is expected to be very weak. In normal RRS spectroscopy on SWNT's, an increase in the temperature results in a higher population of these vibrational levels and makes it possible to obtain measurable anti-Stokes spectra.<sup>13</sup> However, in SERRS, the strong thermal coupling of the nanotubes to the metal substrate prevents the occurrence of such an increase in the temperature. But at extremely strong SERRS enhancement levels, the Raman Stokes process measurably populates the first excited vibrational level in excess of the Boltzmann population. This results in a strong anti-Stokes SERRS spectrum measured at 830-nm (1.49-eV) excitation.<sup>7</sup> Figure 6(b) shows a line-shape analysis of RRS and SERRS Stokes and anti-Stokes spectra of the tangential band measured at this excitation wavelength. In contrast to the Stokes spectra at 1.49 eV discussed above, where RRS and SERRS spectra show similar line-shapes characteristic of semiconducting nanotubes, changes in relative intensities are seen in the anti-Stokes side of the Raman spectra, where so-called preresonance effects involving the *scattered* photon can occur.<sup>7</sup> Although the energy of the incident photon (1.49 eV) is lower than the energy of the  $E_{11}^M(d_1)$  electronic transition associated with the

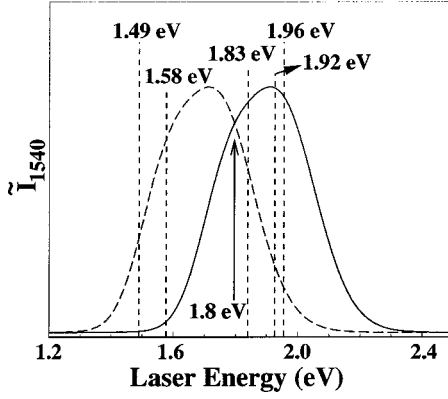


FIG. 7. Metallic window for carbon nanotubes with diameters of  $d_t = 1.35 \pm 0.20$  nm for the Stokes (solid line) and anti-Stokes (dashed line) processes, which cross at  $E_{\text{laser}} = 1.80$  eV (Ref. 13). Also indicated on the figure by vertical dashed lines are  $E_{\text{laser}}$  values used in this study.

metallic nanotubes (thus preventing any resonant Raman enhancement for metallic nanotubes in the Stokes spectra), the upshifted *scattered* anti-Stokes photon gives rise to a resonant Raman effect for metallic nanotubes through the  $E_{11}^M(d_t)$  electronic transition, as shown in Fig. 7, where the expected intensities of the  $1540\text{-cm}^{-1}$  feature for the Stokes process (solid curve) and for the anti-Stokes process (dashed curve) are plotted for SWNT's with diameters  $d_t = 1.35 \pm 0.20$  nm.<sup>13</sup>

It is very interesting to note that while the Stokes spectra at  $E_{\text{laser}} = 1.49$  eV show only vibrational modes associated with the semiconducting nanotubes and no measurable scattering intensity from metallic nanotubes (see Fig. 1), the anti-Stokes spectra in the tangential phonon region, for both the RRS and SERRS spectra can be fitted, using only Lorentzian components associated with metallic nanotubes and no measurable scattering intensity for semiconducting nanotubes, as shown in Table II. The anti-Stokes spectra obtained at  $E_{\text{laser}} = 1.49$  eV (Fig. 6) are therefore in a very special resonance condition, allowing discussion of the differences in the observed RRS and SERRS line shapes when only metallic nanotubes appear to contribute to the anti-Stokes Raman signal. This condition is not observed in the Stokes spectra for our sample, for any of the available laser wavelengths. The different spectral RRS profiles between the Stokes and anti-Stokes Raman spectra are discussed in detail in Ref. 13. The fact that, for the same laser wavelength, the Stokes and anti-Stokes spectra can be in a completely different (metallic vs semiconducting nanotube) regime can be understood in terms of resonance Raman theory and the exceptional elec-

TABLE II. Relative intensities and FWHM linewidths ( $\Gamma$ ) for Lorentzian fits to the RRS and SERRS anti-Stokes spectra for metallic ( $m$ ) nanotube components at  $E_{\text{laser}} = 1.49$  eV.

$\omega$ ( $\text{cm}^{-1}$ )	RRS <sup>a</sup>	$\Gamma$ ( $\text{cm}^{-1}$ )	SERS <sup>a</sup>	$\Gamma$ ( $\text{cm}^{-1}$ )
1515 $m$	0.3	80	0.5	88
1540 $m$	0.6	47	1.2	52
1581 $m$	1.0	34	1.0	43

<sup>a</sup>Intensities relative to  $1581\text{ cm}^{-1}$ .

tronic structure of metallic and semiconducting nanotubes (see Fig. 1). However, if the incident photon may be in weak resonance with the  $E_{11}(d_t)$  transitions, while the scattered photon may be in a much stronger resonance condition, then RRS enhancement can occur through resonance with the scattered photon. Since the resonant enhancement factors can be large ( $> 10^2$ ), it is possible for the scattered photon to dominate the resonance enhancement process, thereby allowing a given  $E_{\text{laser}}$  excitation to probe either metallic or semiconducting nanotubes very selectively, and resulting in very different line shapes at the Stokes and anti-Stokes sides. Such effects are clearly seen in Figs. 4 and 6(b).

We can account for this observation in the following way. Each of the  $1515\text{-}$ ,  $1541\text{-}$ , and  $1581\text{-cm}^{-1}$  Lorentzian components associated with metallic nanotubes will, in general, correspond to different normal-mode displacements and symmetries. The equation for the Raman scattering intensity for each of the Lorentzian components of the ensemble of metallic nanotubes that is involved in the resonant Raman process can be written as

$$I_M = \sum A \exp\left\{\frac{-(d_t - d_0)^2}{\Delta d^2/4}\right\} \left\{ [E_{11}^M(d_t) - E_{\text{laser}} \pm E_{\text{ph}}]^2 + \Gamma_e^2/4 \right\}^{-1} \left\{ [E_{11}^M(d_t) - E_{\text{laser}}]^2 + \Gamma_e^2/4 \right\}^{-1} \quad (1)$$

in which  $I_M \equiv I_M(E_{\text{laser}}, d_t)$  is the scattering intensity for the Stokes process (+ sign) and for the anti-Stokes process (− sign) for each Lorentzian component of the ensemble of metallic nanotubes in resonance with the  $E_{11}^M(d_t)$  electronic transition between the highest lying valence-band van Hove singularity and the lowest lying conduction-band singularity in their 1D electronic density of states.<sup>1,3</sup> The sum in Eq. (1) is over all metallic nanotubes having a diameter distribution given by  $d_t = d_0 \pm \Delta d$  where  $d_0$  is the average diameter and  $\Delta d$  is the full width at half maximum (FWHM) of a Gaussian distribution of nanotube diameters. Also  $E_{\text{ph}}$  denotes the phonon frequency for the tangential band (0.20 eV),  $\Gamma_e$  is a damping parameter determined by fitting experimental data to Eq. (1),  $A$  is a dimensionless factor proportional to the Boltzmann factor  $\exp(-E_{\text{ph}}/kT)$  for the anti-Stokes process and a constant for the Stokes process,<sup>3,16</sup> and the magnitude of this factor  $A$  depends on the scattering cross section for the normal-mode displacements and symmetry of a given vibrational mode.

Equation (1) applies to each Lorentzian component individually. For example, Fig. 7 shows the calculated intensity for the  $1540\text{-cm}^{-1}$  Lorentzian component (the strongest component in the Raman spectra for metallic nanotubes) as a function of  $E_{\text{laser}}$  for the Stokes and anti-Stokes RRS processes. Each component ( $1515$ ,  $1540$ , and  $1581\text{ cm}^{-1}$ ) has a somewhat different intensity profile, which also differs for RRS relative to SERRS. Therefore the composite spectrum that is observed for the tangential modes after summing over the contributions from each nanotube in the sample may show different enhancements for the various Lorentzian components as a function of  $E_{\text{laser}}$ .

For the metallic nanotubes, which are observed in the anti-Stokes spectrum at  $E_{\text{laser}} = 1.49$  eV,<sup>7,13</sup> the RRS spectra and the SERRS spectra, taken with nanotubes adsorbed on the colloidal Ag particles, are also consistent with the corre-

TABLE III. Wave numbers ( $\omega$ ) and FWHM ( $\Gamma$ ) (both given in  $\text{cm}^{-1}$ ) for the second-order  $G'$  Raman band observed at the indicated wavelengths for resonant Raman and SERS spectra.

Spectra	514.5 nm		632.8 nm		647.1 nm	
	$\omega$	$\Gamma$	$\omega$	$\Gamma$	$\omega$	$\Gamma$
RRS	2662	63	2600	68	2604	66
SERS (Au)	2674	56	2624	51	2623	48
SERS (Ag)	2676	54	2624	49	2622	47

sponding results observed at  $E_{\text{laser}} = 1.96, 1.92, \text{ and } 1.83 \text{ eV}$  for the Stokes process on Ag and Au film substrates. The same peak frequencies for the three components for the tangential modes for metallic nanotubes, 1515, 1541, and 1580  $\text{cm}^{-1}$ , that give a good fit to the observed Raman band in the anti-Stokes spectra for both the RRS and SERRS spectra at 1.49 eV, also give a good fit to the Stokes spectra at 1.83, 1.92, and 1.96 eV for the Stokes RRS and SERRS spectra at  $E_{\text{laser}}$  between 1.83 and 1.96 eV.

A more detailed comparison of the relative intensities of each of these components associated with metallic nanotubes in the anti-Stokes spectra at 1.49 eV is given in Fig. 6 and in Table II. Also for the anti-Stokes spectrum at 1.49 eV, for which the metallic nanotubes dominate, the 1541- and 1515- $\text{cm}^{-1}$  components are the ones that are most enhanced by SERRS.

### B. Other Raman bands

In addition to changes in the tangential vibrational modes, other features in the Raman spectra for SWNT's are also perturbed by the presence of the metal substrate (see Fig. 3). In this figure, we see that the  $D$ -band feature (1307–1315  $\text{cm}^{-1}$ ) in the first-order Stokes spectrum at 1.96 eV is upshifted by 4–8  $\text{cm}^{-1}$  in the SERRS spectrum relative to the RRS spectrum, while the corresponding second-order  $G'$  band is upshifted by 24  $\text{cm}^{-1}$  upon interaction with the metal substrate. The data in Table III for the  $G'$  band at three values of  $E_{\text{laser}}$  [2.41 eV (514.5 nm), 1.96 eV (632.8 nm), 1.92 eV (647.1 nm)] show that the shift in the  $G'$  band is much larger for  $E_{\text{laser}}$  values where *metallic* nanotubes contribute strongly to the Raman spectra than for the  $E_{\text{laser}}$  value in the semiconducting regime.

Furthermore, at  $E_{\text{laser}} = 1.96 \text{ eV}$  (within the metallic window), the intensity of the  $G'$  band relative to that of the tangential mode, denoted simply by  $(I_{G'}/I_{\text{tang}})$ , has a value of 0.4 for the normal Raman spectra as compared to a significantly larger value of 0.6 for the SERS spectra. In contrast, for  $E_{\text{laser}} = 2.41 \text{ eV}$  where only semiconducting nanotubes are in resonance with  $E_{\text{laser}}$ , the ratio  $(I_{G'}/I_{\text{tang}})$  has the same value of 0.2 for both the NRS and SERS spectra.

Figure 6 for  $E_{\text{laser}} = 1.49 \text{ eV}$  also shows a large upshift in the frequency of the second-order  $G'$  band for the adsorbed nanotubes (from 2600  $\text{cm}^{-1}$  for the normal resonant Raman spectrum to 2636  $\text{cm}^{-1}$  for the SERRS spectrum) at the *anti-Stokes* side of the Raman spectra. For the anti-Stokes spectra which is dominated by resonance with metallic nanotubes, the relative intensities of the  $G'$  band to the tangential band seems to be a factor of  $\sim 2$  larger for the RRS spectrum relative to the SERS spectrum which can be explained by

laser heating of the samples in RRS. Such heating does not, however, appear for SERRS because of the good thermal contact between the nanotubes and the metal substrates. It should also be mentioned that the optical pumping effect, which can account for the strong anti-Stokes spectrum,<sup>7</sup> is expected to be very weak at the high phonon energy of  $\sim 2600 \text{ cm}^{-1}$ . Further study is necessary to understand this effect in more detail. In summary, the intensities in the SERS Stokes spectra of the  $G'$  band are larger relative to the tangential vibrational band for the metallic single-wall carbon nanotubes, in contrast to the situation for the semiconducting nanotubes where the intensity ratios are the same for all  $E_{\text{laser}}$  values that were studied.

The  $(\omega_{\text{tang}} + \omega_{\text{RBM}})$  and  $(\omega_{\text{tang}} + 2\omega_{\text{RBM}})$  combination band frequencies at 1730 and 1905  $\text{cm}^{-1}$ , respectively, in the RRS spectrum in Fig. 3 are also upshifted to 1740 and 1931  $\text{cm}^{-1}$ , respectively, for the adsorbed nanotubes in the corresponding SERRS spectra at 1.96 eV. It is interesting to note that the larger upshift for the  $(\omega_{\text{tang}} + 2\omega_{\text{RBM}})$  combination mode is consistent with the larger variation of this mode frequency with  $E_{\text{laser}}$  in the RRS spectra.<sup>16</sup> This phenomenon is under further investigation.

Since the mechanism responsible for resonant Raman scattering for the  $D$  band in the first-order spectrum and for the  $G'$  band in the second-order spectrum at twice the  $D$ -band frequency is quite different from that for the tangential band,<sup>18</sup> a comparison of the behavior of these modes under normal resonant Raman scattering and under SERRS yields valuable information about these phenomena. From the above discussion on the tangential mode spectra, we conclude that the same Lorentzian components appear in the line-shape analysis of the RRS and the SERRS spectra for the semiconducting nanotubes (at 1563, 1591, and 1601  $\text{cm}^{-1}$ ) without change in the relative intensities of these Lorentzian components. And even in the RRS and SERRS spectra for the *metallic* nanotubes, the same Lorentzian components (1515, 1540, and 1581  $\text{cm}^{-1}$ ) appear in both the RRS and SERRS spectra, though with different relative intensities at a given value of  $E_{\text{laser}}$ . From these results, we conclude that the normal-mode vibrations are essentially unchanged by the interaction between the nanotubes and the metal substrate. But rather the electronic excitations are somewhat perturbed by this interaction, with evidence for this interpretation coming from the upshift in the  $D$ -band and the  $G'$ -band frequencies in the SERRS spectra for all nanotubes relative to the corresponding RRS spectra, and from the relative increase in the intensities of these Raman bands in the SERRS spectra for the metallic nanotubes. Following this line of reasoning, we argue that the interaction between the nanotubes and the metal substrate perturbs the electronic structure near the  $K$  point of the 2D graphene Brillouin zone, so that the  $D$ -band and the  $G'$ -band vibrational spectra which are resonantly excited by a given laser energy  $E_{\text{laser}}$  now correspond to a slightly upshifted  $k$  point relative to the  $K$  point in the 2D Brillouin zone. But since the  $D$ -band (and the  $G'$ -band) phonon that is resonantly enhanced has the same wave vector as that of the resonant electronic transition,<sup>18</sup> the upshift in the SERRS spectrum relative to the RRS spectrum is a measure of the strength of the electronic interaction between the nanotube and the metal substrate. Because of the much larger experimentally observed

upshift of the  $G'$ -band frequency for the *metallic* nanotubes, we conclude that the interaction of the metallic nanotubes with the metal substrate is much stronger than for the semiconducting nanotubes. This conclusion is also consistent with the increased intensity of the Lorentzian components associated with the tangential band of metallic nanotubes in the SERRS spectra relative to the intensity of the same Lorentzian components in the RRS spectra. These arguments also lead to the conclusion that the electron-phonon interaction is stronger for the metallic nanotubes than for the semiconducting nanotubes.

Surface-enhanced resonant Raman spectroscopy predominantly enhances the symmetric vibrations for the nanotubes. The large upshift in the  $G'$  band for metallic nanotubes in the SERRS spectra (by  $\sim 24\text{ cm}^{-1}$ ) for  $E_{\text{laser}}=1.96\text{ eV}$ , and for the semiconducting nanotubes (by  $\sim 13\text{ cm}^{-1}$ ) at  $E_{\text{laser}}=2.41\text{ eV}$  is consistent with the “breathing-mode”-type motion of the carbon atoms for the mixed “quasiacoustic” optic phonon branch near the  $K$  point.<sup>18</sup> Normal resonant Raman and SERS spectral intensities are both larger for the totally symmetric modes, and the very appearance of the  $G'$  band in the Raman spectra relies greatly on the “breathing-type” motion of the phonons involved.<sup>18</sup> The larger shift in the  $G'$  band in the SERS spectra for the metallic nanotube regime (which includes spectra taken at both 1.96 and 1.92 eV) would also be an indication of a stronger interaction of the metallic nanotubes with the metal substrate reflected in the greater SERS enhancement for the metallic nanotubes, while the smaller shift for the semiconducting nanotubes is consistent with a lesser SERS enhancement due to a smaller interaction between semiconducting nanotubes and the metal substrate. The frequency upshift observed for the combination bands ( $\omega_{\text{tang}} + \omega_{\text{RBM}}$  and  $\omega_{\text{tang}} + 2\omega_{\text{RBM}}$ ) also supports the argument that the combination modes contain a totally symmetric mode in the decomposition of the direct product of the symmetry types contained in the combination mode.

### C. SERS enhancement mechanism

There are two major contributions to the surface enhancement of the resonant Raman scattering of carbon nanotubes adsorbed on metallic surfaces: the “electromagnetic” mechanism and the “chemical” mechanism, based on a charge transfer between the metallic surface and the nanotubes. The “electromagnetic” mechanism is due to the enhanced electromagnetic fields at or near nanometer size metallic particles, in our case “rough” silver and gold surfaces. Particularly strong field enhancement up to 10 to 12 orders of magnitude can exist for metallic substrates showing fractal cluster structures.<sup>22–24</sup> At the applied excitation wavelengths in the reported experiments, the electromagnetic enhancement is expected to be based on resonances of the optical fields with the collective electronic excitations of such cluster structures and not with those of the isolated particles. This “cluster-based” field enhancement does not directly depend on the sizes and shapes of the individual particles, and therefore is expected to be similar for our metal island films and colloidal silver surfaces. The fields that are highly localized in small areas of the cluster<sup>23</sup> result in much stronger SERRS enhancement for clusters than for

isolated particles.<sup>25,26</sup> Theoretical calculations predict that these SERS-active substrates should exhibit a particularly strong enhancement at longer wavelength (near-infrared) excitation.<sup>24</sup> In general, the electromagnetic enhancement mechanism is independent of the chemical nature of the species, and is also expected to be the same for all vibrational modes. The existence of such large enhancement levels has been shown for both semiconducting and metallic nanotubes.<sup>7</sup> The second enhancement mechanism, the charge-transfer or chemical effect, strongly depends on the electronic structure of the nanotubes, and this mechanism should sensitively differentiate between the very different 1D density of states between the metallic and semiconducting nanotubes.

For Raman Stokes spectra within the semiconducting regime ( $E_{\text{laser}}=1.58$  and  $2.41\text{ eV}$ ), no significant dependence of the SERRS spectra is observed on the metal species (silver or gold), nor on the metal film thickness for a given  $E_{\text{laser}}$  value. In the semiconducting nanotube regime, all SERRS bands are enhanced by the same amount, as expected from the electromagnetic enhancement mechanism.

For laser excitation energies within the metallic resonance window, however, we observe an enhanced contribution to the SERRS spectra of selected Lorentzian components (at  $1540$  and  $1515\text{ cm}^{-1}$ ), associated with metallic nanotubes. We explain this effect in terms of a charge-transfer enhancement, which is operative for the metallic nanotubes, in addition to the strong electromagnetic field effect discussed above. The different behavior between the SERRS spectra of metallic and semiconducting nanotubes arises from the major differences in their electronic structures, in their 1D density of states near the Fermi level, and from their stronger electron-phonon coupling in metallic as compared to semiconducting nanotubes.

It is well established that the chemical mechanism of enhancement can be described as a resonant Raman effect involving electronic levels of the substrate and of the adsorbed molecules as well. The chemical effect therefore depends on the occurrence of a resonance condition between the laser energy and the energy separation of the van Hove singularities in the 1D peaks of the electronic density of states of the nanotube adsorbate, as modified by interaction with the metal substrate.

Furthermore, the selection rules for the charge-transfer mechanism predict that modes with different symmetries and with different vibrational normal-mode displacements should behave differently, just as for the resonant Raman selection rules.<sup>27,28</sup> In particular, totally symmetric modes are more likely to be enhanced through the Franck-Condon mechanism in both SERS and resonant Raman spectroscopies.<sup>29</sup> The fitted data in Fig. 5 indicate that the different tangential Lorentzian components identified with the metallic nanotubes are enhanced by different amounts, with a preferential enhancement of the  $1540\text{-cm}^{-1}$  component. Both the RRS and SERRS spectra indicate that the strongly enhanced  $1540\text{-cm}^{-1}$  vibrational component is the one that is more likely to have predominantly  $A_{1g}$  symmetry, though a convincing identification awaits definitive polarization measurements.<sup>30</sup>

#### IV. CONCLUSIONS

In this paper, we have studied in detail the surface enhancement of resonance Raman scattering of SWNT's on silver and gold nanostructures. By looking at small changes between the RRS and SERRS spectra at various laser excitation energies for selected modes of the metallic nanotubes, we have found a small contribution of "chemical" SERRS enhancement to the very strong total enhancement factor inferred in previous work.<sup>7</sup> This finding is in agreement with RRS studies, which also show a stronger electron-phonon coupling for the metallic nanotubes as compared to the semiconducting nanotubes. Therefore changes in the electronic states which appear through interaction between the nanotubes and the metal substrate show up as changed SERRS conditions for observing the related phonon bands. In principle, the electronic states for semiconducting nanotubes might also be changed by the interaction of the nanotubes with the metal substrate. Wildöer *et al.* have reported<sup>31</sup> an interaction effect (resulting in a shift of the electronic density of states) between carbon nanotubes in contact with a smooth gold substrate in their scanning tunneling microscopy/spectroscopy (STM/STS) study of the electronic density of states in carbon nanotubes. However, due to the weaker electron-phonon coupling for semiconducting nanotubes, the surface interaction effect is too weak to be monitored in the SERRS spectra of the semiconducting nanotubes, except through our observations of a small upshift ( $13\text{ cm}^{-1}$ ) in the  $G'$ -band frequency for semiconducting nanotubes, compared to the larger ( $24\text{ cm}^{-1}$ ) upshift for the metallic nanotubes. Therefore, the fact that we did not find a charge-transfer

contribution to SERRS from the tangential mode in the semiconducting nanotubes does not prove that there is no electronic interaction between these tubes and the metal substrate. Because of the weaker electron-phonon coupling in semiconducting nanotubes, SERRS is simply not a sensitive enough tool to look for changes in their electronic states. But, our independent probe of measuring the upshift of the  $G'$  band in SERS, indicates a stronger interaction of the electronic states of the metallic nanotubes with the metal substrate than for the semiconducting nanotubes. The selective enhancement of modes which can be assigned to a totally symmetric mode (such as the  $1540\text{-cm}^{-1}$  mode in our case) is in agreement with RRS and SERRS studies of molecules.<sup>29</sup>

#### ACKNOWLEDGMENTS

The authors are thankful to Dr. Gene Hanlon, K. Shafer, and J. Motz for their help with the measurements, and we gratefully acknowledge support for this work under NSF Grant No. DMR 98-04734. M.A.P. would like to acknowledge support by the Brazilian agencies FAPEMIG, CAPES, and FINEP. P.C. would like to acknowledge support by the Brazilian agency FAPESP. K.K. would like to thank Professor M.S. Feld and Dr. R.R. Dasari for their kind hospitality and support of this research, and for many stimulating discussions. The measurements performed at the George R. Harrison Spectroscopy Laboratory at MIT were supported by the NIH Grant No. P41-RR02594 and NSF Grant No. CHE9708265.

<sup>1</sup>M. S. Dresselhaus, G. Dresselhaus, and P. C. Eklund, *Science of Fullerenes and Carbon Nanotubes* (Academic Press, New York, 1996).

<sup>2</sup>R. Saito, G. Dresselhaus, and M. S. Dresselhaus, *Physical Properties of Carbon Nanotubes* (Imperial College Press, London, 1998).

<sup>3</sup>M. A. Pimenta, A. Marucci, S. Empedocles, M. Bawendi, E. B. Hanlon, A. M. Rao, P. C. Eklund, R. E. Smalley, G. Dresselhaus, and M. S. Dresselhaus, *Phys. Rev. B* **58**, R16016 (1998).

<sup>4</sup>A. M. Rao, E. Richter, S. Bandow, B. Chase, P. C. Eklund, K. W. Williams, M. Menon, K. R. Subbaswamy, A. Thess, R. E. Smalley, G. Dresselhaus, and M. S. Dresselhaus, *Science* **275**, 187 (1997).

<sup>5</sup>K. Kneipp, Y. Wang, H. Kneipp, I. Itzkan, R. R. Dasari, and M. S. Feld, *Phys. Rev. Lett.* **76**, 2444 (1996).

<sup>6</sup>K. Kneipp, Y. Wang, H. Kneipp, L. T. Perelman, I. Itzkan, R. R. Dasari, and M. S. Feld, *Phys. Rev. Lett.* **78**, 1667 (1997).

<sup>7</sup>K. Kneipp, H. Kneipp, P. Corio, S. D. M. Brown, K. Shafer, J. Motz, L. T. Perelman, E. B. Hanlon, A. Marucci, G. Dresselhaus, and M. S. Dresselhaus, *Phys. Rev. Lett.* (in press).

<sup>8</sup>G. S. Duesberg, W. J. Blau, H. J. Byrne, J. Muster, M. Burghard, and S. Roth, *Chem. Phys. Lett.* **310**, 8 (1999).

<sup>9</sup>A. Otto, I. Mrozek, H. Grabhorn, and W. Akemann, *J. Phys.: Condens. Matter* **4**, 1143 (1992).

<sup>10</sup>M. Moskovits, *Rev. Mod. Phys.* **57**, 783 (1985).

<sup>11</sup>A. Campion, J. E. Ivanecky III, C. M. Child, and M. J. Foster, *J.*

*Am. Chem. Soc.* **117**, 11 807 (1995).

<sup>12</sup>A. Campion and P. Kambhampati, *Chem. Soc. Rev.* **27**, 241 (1998).

<sup>13</sup>S. D. M. Brown, P. Corio, A. Marucci, M. S. Dresselhaus, M. A. Pimenta, and K. Kneipp, *Phys. Rev. B* **61**, R5137 (2000).

<sup>14</sup>P. C. Lee and D. Meisel, *J. Phys. Chem.* **86**, 3391 (1982).

<sup>15</sup>G. Mie, *Ann. Phys. (Leipzig)* **25**, 377 (1908).

<sup>16</sup>S. D. M. Brown, P. Corio, A. Marucci, M. A. Pimenta, M. S. Dresselhaus, and G. Dresselhaus, *Phys. Rev. B* **61**, 7734 (2000).

<sup>17</sup>M. S. Dresselhaus, M. A. Pimenta, K. Kneipp, S. D. M. Brown, P. Corio, A. Marucci, and G. Dresselhaus, in *Science and Applications of Nanotubes*, edited by D. Tománek and R. J. Ebody (Kluwer Academic, New York, 2000), p. 253.

<sup>18</sup>M. J. Matthews, M. A. Pimenta, G. Dresselhaus, M. S. Dresselhaus, and M. Endo, *Phys. Rev. B* **59**, R6585 (1999).

<sup>19</sup>M. J. Matthews, M. A. Pimenta, S. D. M. Brown, A. Marucci, M. S. Dresselhaus, M. Endo, and C. Kim (unpublished).

<sup>20</sup>H. Kataura, Y. Kumazawa, N. Kojima, Y. Maniwa, I. Umezumi, S. Masubuchi, S. Kazama, X. Zhao, Y. Ando, Y. Ohtsuka, S. Suzuki, and Y. Achiba, *Synth. Met.* **103**, 2555 (1999).

<sup>21</sup>H. Kataura, Y. Kumazawa, Y. Maniwa, I. Umezumi, S. Suzuki, Y. Ohtsuka, and Y. Achiba, *Synth. Met.* **103**, 2555 (1999).

<sup>22</sup>V. M. Shalaev and M. I. Stockman, *Zh. Éksp. Teor. Fiz. [Sov. Phys. JETP]* **65**, 287 (1987).

<sup>23</sup>V. A. Markel, V. M. Shalaev, P. Zhang, W. Huynh, L. Tay, T. L. Haslett, and M. Moskovits, *Phys. Rev. B* **59**, 10 903 (1999).

- <sup>24</sup>M. I. Stockman, V. M. Shalaev, M. Moskovits, R. Botet, and T. F. George, *Phys. Rev. B* **46**, 2821 (1992).
- <sup>25</sup>K. Kneipp, H. Kneipp, V. B. Kartha, R. Manoharan, G. Deinum, I. Itzkan, R. R. Dasari, and M. S. Feld, *Phys. Rev. E* **57**, R6281 (1998).
- <sup>26</sup>K. Kneipp, H. Kneipp, R. Manoharan, E. B. Hanlon, I. Itzkan, R. R. Dasari, and M. S. Feld, *Appl. Spectrosc.* **527**, 1493 (1998).
- <sup>27</sup>J. R. Lombardi, R. L. Birke, T. H. Lu, and J. Xu, *J. Chem. Phys.* **84**, 4174 (1986).
- <sup>28</sup>P. Corio, J. C. Rubim, and R. Aroca, *Langmuir* **14**, 4162 (1998).
- <sup>29</sup>R. J. H. Clark and T. J. Dines, *Angew. Chem.* **25**, 131 (1986).
- <sup>30</sup>A. M. Rao, A. Jorio, M. A. Pimenta, M. S. S. Dantas, R. Saito, G. Dresselhaus, and M. S. Dresselhaus, *Phys. Rev. Lett.* **84**, 1820 (2000).
- <sup>31</sup>J. W. G. Wildöer, L. C. Venema, A. G. Rinzier, R. E. Smalley, and C. Dekker, *Nature (London)* **391**, 59 (1998).
- <sup>32</sup>G. Dresselhaus, M. A. Pimenta, R. Saito, J.-C. Charlier, S. D. M. Brown, P. Corio, A. Marucci, and M. S. Dresselhaus, in *Science and Applications of Nanotubes*, edited by D. Tománek and R. J. Enbody (Kluwer Academic, New York, 2000), p. 275.
- <sup>33</sup>R. Saito, G. Dresselhaus, and M. S. Dresselhaus, *Phys. Rev. B* **61**, 2981 (2000).